ISSN: 0975-8585

Research Journal of Pharmaceutical, Biological and Chemical Sciences

New Au (III), Pd (II), Cu (II), Fe (II) and Mn (II) complexes containing O, N-donor Schiff base ligand derived from 1-Hydroxy-2-acetonaphthone and 4-Chlorophenyl ethylamine: synthesis, spectral analysis and biological relevance.

D V Bondar*.

Department of Chemistry, B.S.S. College, Makni, Tal. Lohara, Dist. Dharashiv, Maharashtra, India.

ABSTRACT

The present work deals with the synthesis, characterization and biological properties of five novel Au (III), Pd (II), Cu (II), Fe (II) and Mn (II) Schiff base complexes with(E)-2-(1-((4-chlorophenethyl) imino) ethyl) naphthalen-1-ol (HL). The synthesized metal complexes have been explored using UV-visible, magnetic moment, molar conductance, FT-IR, ^{1}H NMR, LCMS and powder X-ray diffraction. Interestingly, the interactions between metal ions and ligand occurring deprotonated oxygen and Schiff base imine nitrogen have been demonstrated and analysed using FT-IR, NMR and XRD. The geometries of the metal complexes Au (III) and Pd (II) are square planar, whereas Cu (II) complex is distorted square planar and Fe (II) and Mn (II) complexes have octahedral geometry. Metal complexes are tested *in vitro* for antibacterial activity against gram-negative bacteria *E. coli, P. aeruginosa* and gram-positive *S. aureus, B. subtilis* as well as antifungal activity against the two fungi *C. albicans* and *A. niger*. According to biological studies, metal complexes are more effective than non-complexed ligand against bacterial and fungal species. Interestingly, Pd(II) complexes have extremely high antioxidant activity, whereas Au (III) and Mn (II) complexes have moderate to strong antioxidant activity.

Keywords: 4-Chlorophenylethyl amine, 1-Hydroxy-2-acetonaphthone, Schiff base complex, ^{1}H-NMR, Anti-microbial, Anti-oxidant

Graphical abstract

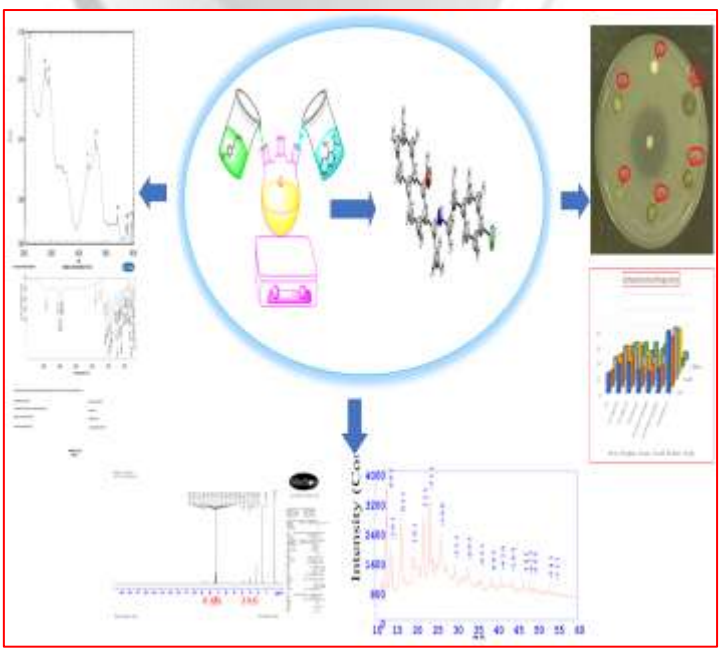

https://doi.org/10.33887/rjpbcs/2026.17.4.5

Corresponding author

ISSN: 0975-8585

INTRODUCTION

Currently, an essential medical concern is the increasing resistance of bacteria against usually available antibiotics which lead to the production of new pioneering antimicrobial compounds that can be proved to have potential beside these rehabilitated infections [1, 2]. Schiff bases are an outstanding topic for the simple investigation with an essential place in organic chemistry and a wide range of applications. They have several physiological applications as antitumor agents, in the reinforcement of immune response for cancer, leukaemia, anti-HIV, anticonvulsant, antibacterial, antifungal, anti-inflammatory, prodrugs [3]. There are several names for the species comportment imine bonds (–C=N–) including imines, anils, Schiff bases and azomethines. These compounds can be effortlessly formed by the condensation of primary amines with aldehydes or ketones in a convinced solvent [4]. These moieties are effective as chelating materials because of their structural modification, easy method of synthesis and have adequately of applications in industry and medicine [5-7]. Schiff base complexes or scaffolds have a broad scope in the physiological and chemical reactions as a catalyst [8], dye and pigments [9, 10], in polymerization and fluorescence [11, 12], organic light emitting devices (OLED) [13]. Schiff bases covering the heteroatoms O, N and S create bioactivities like as antimicrobial [14, 15], antimalarial [16], antitumor [17], anticancer [18], antiviral [19], anti-HIV [20], anticonvulsant activity [21], anticovid [22].

However, the 1-hydroxy-2-acetonaphthone (HAN) motif's Schiff bases offer a wide range of medical applications. Bioactivities are created by different Schiff bases using naphthalene scaffolds, which is exceptional in drug discovery [23]. Naphthalene and di-imide Schiff bases, as well as naphthospiro chromanone scaffolds, have been shown to have antiproliferative effects on several types of tumour cells [24, 25]. Similarly, the HAN Schiff base has antimicrobial and antioxidant properties [26], beginning with HAN naphthoflavones, which are potent antihyperuricemic agents [27].

Furthermore, there is a huge collection of biogenic amines, which are arylalkyl amines with a high value due to their unique configuration and amazing biological functions such as antifungal [28], anti-inflammatory [29], anticancer, and antioxidant [30]. The Phenylethyl amine motif is a monoamine alkaloid including both a psychoactive drug and an effective stimulant [31]. Arylalkyl amines have an important role in the human nervous system [32] and also function as prodrugs [33]. 4-Methoxyphenyl ethylamine and other ethyl amine analogues are used as anti-HIV drugs [34]. Phenylethyl amine has no substantial central action when delivered systemically at low doses, but minor structural adjustments have a considerable impact on its pharmacology, resulting in a vast number of valuable pharmacological tools. As a result, phenylethyl amine has therapeutic potential in the treatment of drugs of abuse such as hallucinogens, CNS stimulants, and empathogens [35]. 4-Chlorophenyl ethylamine Schiff base has high antibacterial activity [36]. Chlorophenyl ethylamine's urea counterpart penetrates the brain and decreases cocaine-seeking behavior reinstatement [37]. Furthermore, 4-chlorophenyl ethylamine compounds exhibit anticancer, anti-inflammatory, and analgesic properties [38].

Based on this method, the current work focuses on a specific type of chelating Schiff base produced by condensing 1-hydroxy-2-acetonaphthone and 4-chlorophenylethyl amine in a 1:1 ratio. Schiff base ligands have a coordination number of two (O, N), allowing them to chelate with metal ions in a 2:1 ratio and form complexes with Au (III), Pd (II), Cu (II), Fe (II), and Mn (II) transition metal ions via two covalent and two coordinate covalent interactions. In order to investigate the structure of the synthesized Schiff base ligand and complexes have been investigated using FT-IR, UV-Vis, ^{1}H and ^{13}C NMR, SC-XRD, LCMS spectroscopic study and other structural techniques. Additionally, biological activity assessments are conducted to assess the compounds antioxidant and antibacterial properties toward *E. Coli, P. aeruginosa, S. aureus* and *B. subtilis* microbes, as well as their antifungal properties against *C. albicans* and *A. niger* fungus.

EXPERIMENTAL

Materials and methods

All chemicals are AR grade, 1-Hydroxy-2-acetonaphthone, 4-Chlorophenylethyl amine, metal acetates and chloride have been bought from Sigma Aldrich. Absolute ethanol, HPLC grade methanol and other solvents were purchased from local sources. All the reaction optimized by TLC Alu foil silica gel 60 F_{254}. Melting points have been determined using a digital apparatus known as the Kofler Bench. The Perkin-Elmer 240 elemental analyzer was used for elemental analysis. The metal complexes UV-Vis

spectra were acquired at 200-600 nm using a Shimadzu UV-1800 240V spectrophotometer using methanol as a solvent. Magnetic susceptibilities were resolute by the Faraday process using a model 300 Lewis coil Force Magnetometer of Tesla strength at ambient temperature. The instrument was standardized using $HgCo(NCS)_4$. The molar conductance of metal complexes in DMF solution was measured using the ELICO CM-82 conductivity Bridge ($1x10^{-3}$M). FT-IR spectra were recorded with KBr pallets on a Bruker Alpha II instrument in the range 650 – 4000 cm^{-1}. ^1H NMR were recorded on Bruker AVANCE NEO 400 MHz spectrometer with $CDCl_3$ solvent and tetramethyl silane (TMS) as an internal reference standard. Compound LCMS mass spectra were obtained using a single quadrupole Agilent 1290 G7104A, model LCMSD G6125B MSD with a scan range of 100m/z to 1400m/z. The powder XRD of ligand and complexes were recorded using a Desktop X- ray Diffractometer MiniFlex II of range 10 – 80 ° target Cu with wavelength λ= 1.540598 Å.

Synthesis of Schiff base ligand (HL)

The preparation of Schiff base ligand was documented in the literature [39]. For this, 1 mM of 1-Hydroxy-2-acetonaphthone (0.186 g) was completely dissolved in 10 mL of hot absolute ethanol which contained 2–3 drops of glacial acetic acid. To this, 10 mL absolute ethanolic 1mM of 4-Chlorophenyl ethylamine (0.156 g) was added with continuous stirring in 100 mL RBF and the reaction solution was refluxed for 3 h (**Scheme 1**). The progress of the reaction was monitored by TLC using an 8:2 solvent mixture of n-hexane-ethyl acetate. After consuming the starting material, the reaction mixture was left at room temperature overnight and the glossy yellow crystals were collected by filtering, washed and recrystallized with absolute ethanol to yield pure Schiff base ligand.

(E)-2-(1-((4-chlorophenethyl)imino)ethyl)naphthalen-1-ol, H**L**; Yield: 0.280 g, 82%. m. p.- 166-168 °C; colour- Greenish-yellow. LCMS: *m/z* $[M]^+$ = 323.82. Anal. Calcd. For $C_{20}H_{18}ClNO$ (%): C, 74.18; H, 5.60; Cl, 10.95; N, 4.33; O, 4.94%. Found: C, 74.10; H, 5.52; Cl, 10.91; N, 4.27; O, 4.89%. FT-IR (KBr, cm^{-1}): 3424.77 (ν OH); 1701.15 (ν C=N); 1591.42- 1455.73 (ν Ar C=C); 1271.88 (ν C-O); 1016.67 (ν C-N-C). ^1H NMR (400 MHz, $CDCl_3$), δ (ppm): 16.465 (s, Ar-OH); 8.524- 6.769 (m, Ar-H); 3.769 (t, N-CH_2); 3.068 (t, -CH_2-Ar); 2.268 (s, -CH_3). ^{13}C NMR (100 MHz, $CDCl_3$), δ (ppm): 175.748 (-C=N-); 170.842 (-C-OH); 136.370 (-C-Cl); 108.331- 137.205 (-Ar-C-); 46.471 (-N=C-); 35.623 (-CH_2-C-Ar); 13.937 (N=C-CH_3). UV-Vis λ_{max} (nm) (CH_3OH): 222; 271.50; 287.50; 322.50; 409.50.

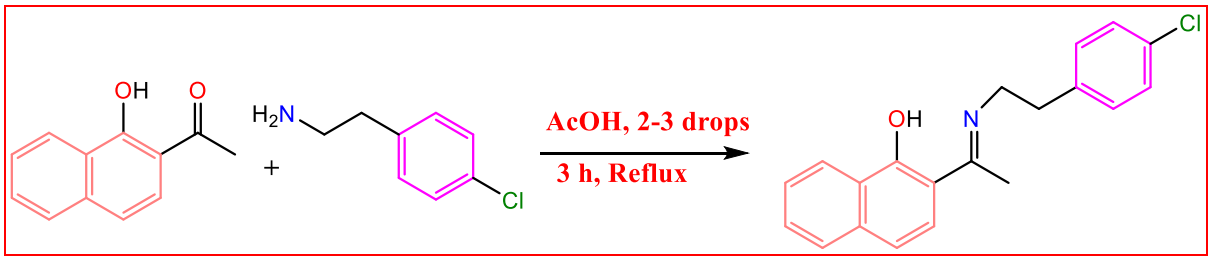

Scheme 1 - Synthesis of Schiff base ligand (HL)

Synthesis of metal complexes [M(L)$_2$]

In order to synthesize metal complexes, 1 mM of each metal salt, $HAuCl_4 \cdot 3H_2O$ (0.393 g), Pd $(OAc)_2$ (0.224 g), Cu $(OAc)_2 \cdot H_2O$ (0.199 g), Fe (II)$(OAc)_2 \cdot 4H_2O$ (0.246 g) and Mn (II)$(OAc)_2 \cdot 4H_2O$ (0.245 g), was each dissolved in 10 mL methanol. To this, hot 15 mL methanolic solution of 2-(1-((4-chlorophenethyl)imino)ethyl)naphthalen-1-ol (H**L**) (2 mM) was added with continuous stirring (**Scheme 2**). The reaction mixture was refluxed for 4-5 h, yielding a coloured precipitate of metal complexes. These precipitates were then filtered, washed thoroughly with methanol and petroleum ether, recrystallized in methanol and dried in an oven.

ISSN: 0975-8585

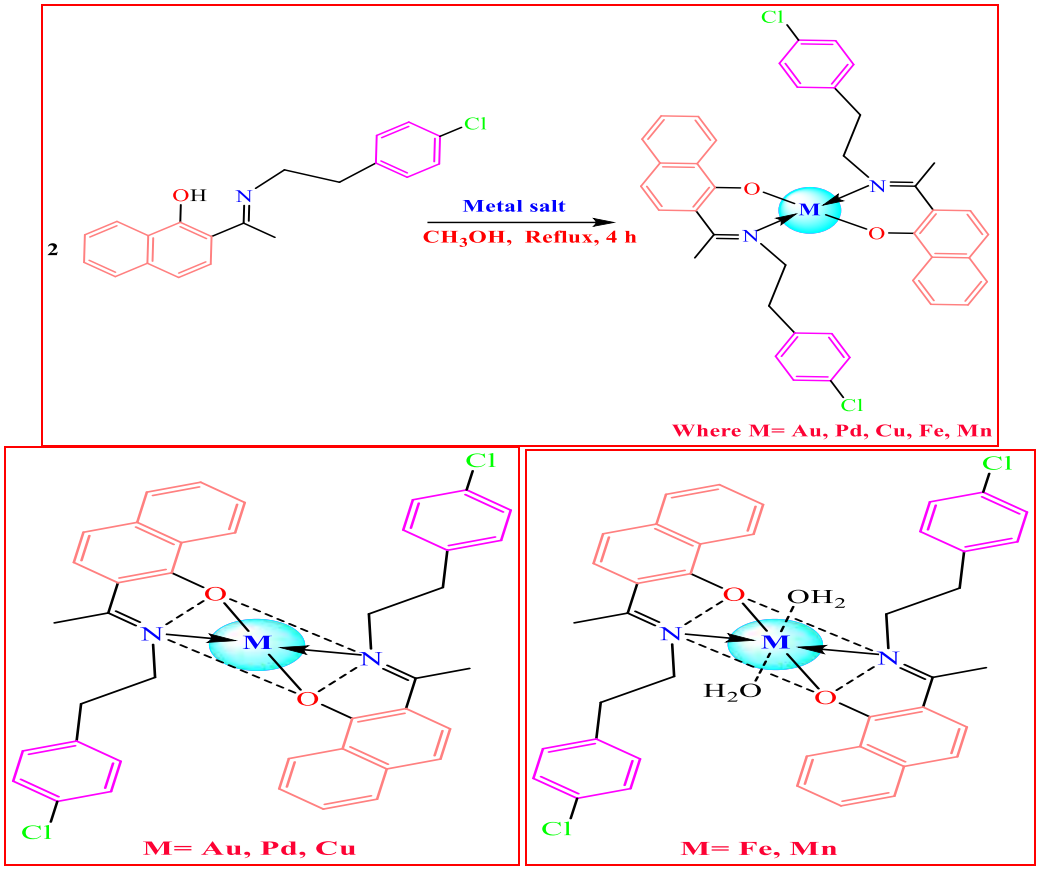

Scheme 2 - Synthesis of complexes $[M(L)_2]$ and its structural shape

$[Au(L)_2]$

Yield: 27%. m. p.- 300< °C; golden. LCMS: *m/z* $[M]^+$ = 842.59. Anal. Calcd. For $C_{40}H_{34}Cl_2N_2O_2Au$: C, 56.98; H, 4.05; N, 3.29; O, 3.76; Cl, 8.38; Au, 23.36% Found: C, 57.02; H, 4.07; N, 3.32; O, 3.80; Cl, 8.41; Au, 23.38%. FT-IR (KBr, cm^{-1}): 1592.27 (ν C=N); 1246.55 (ν C-O); 1020.52 (ν C-N-C). ^1H NMR (400 MHz, $CDCl_3$), δ (ppm): 8.629-6.996 (m, Ar-H); 3.828 (t, N-CH_2); 3.122 (t, -CH_2-Ar); 2.304 (s, -CH_3). UV-Vis λ_{max} (nm) (CH_3OH): 220; 274; 339; 433; 462; 541; 573.

$[Pd(L)_2]$

Yield: 62%. m. p.- 250< °C; Dark brown. LCMS: *m/z* $[M]^+$ = 752.04. Anal. Calcd. For $C_{40}H_{34}Cl_2N_2O_2Pd$: C, 63.85; H, 4.54; N, 3.69; O, 4.23; Cl, 9.38; Pd, 13.98% Found: C, 63.88; H, 4.56; N, 3.73; O, 4.25; Cl, 9.43; Pd, 14.1%. FT-IR (KBr, cm^{-1}): 1618.05 (ν C=N); 1246.19 (ν C-O); 1012.19 (ν C-N-C). ^1H NMR (400 MHz, $CDCl_3$), δ (ppm): 8.282-6.823 (m, Ar-H); 4.276 (t, N-CH_2); 3.343 (t, -CH_2-Ar); 2.309 (s, -CH_3). UV-Vis λ_{max} (nm) (CH_3OH): 214; 243; 287; 322; 372; 437; 484.

$[Cu(L)_2]$

Yield: 78%. m. p.- 250< °C; Brown. LCMS: *m/z* $[M]^+$ = 709.17, Anal. Calcd. For $C_{40}H_{34}Cl_2N_2O_2Cu$: C, 67.72; H, 4.82; N, 3.91; O, 4.48; Cl, 9.97; Cu, 8.93% Found: C, 67.75; H, 4.83; N, 3.95; O, 4.51; Cl, 10.00; Cu, 8.96%. FT-IR (KBr, cm^{-1}): 1618.18 (ν C=N); 1250.17 (ν C-O); 1014.26 (ν C-N-C). ^1H NMR (400 MHz, $CDCl_3$), δ (ppm): 8.953-6.511 (m, Ar-H); 3.818 (t, N-CH_2); 3.097 (t, -CH_2-Ar); 2.314 (s, -CH_3). UV-Vis λ_{max} (nm) (CH_3OH): 221; 271; 286; 328; 407; 436.

$[Fe(L)_2(H_2O)_2]$

Yield: 62%. m. p.- 243-245 °C; Brown red. LCMS: *m/z* $[M]^+$ = 737.50, Anal. Calcd. For $C_{40}H_{34}Cl_2N_2O_2Fe$: C, 65.12; H, 5.15; N, 3.78; O, 8.65; Cl, 9.59; Fe, 8.93% Found: C, 65.14; H, 5.19; N, 3.80; O, 8.68; Cl, 9.61; Cu,

7.57%. FT-IR (KBr, cm^{-1}): 1588.36 (ν C=N); 1271.69 (ν C-O); 1014.88 (ν C-N-C). ^1H NMR (400 MHz, $CDCl_3$), δ (ppm): 8.523-6.799 (m, Ar-H); 3.832 (t, N-CH_2); 3.094 (t, -CH_2-Ar); 2.307 (s, -CH_3). UV-Vis λ_{max} (nm) (CH_3OH): 220; 272; 288; 328; 409; 439.

[Mn(L)$_2$ (H_2O)$_2$]

Yield: 54%. m. p.- 212-214 ^oC; Olive. LCMS: *m/z* $[M]^+$ = 736.59, Anal. Calcd. For $C_{40}H_{34}Cl_2N_2O_2Mn$: C, 65.19; H, 5.16; N, 3.76; O, 8.66; Cl, 9.60; Mn, 7.44% Found: C, 65.22; H, 5.20; N, 3.80; O, 8.69; Cl, 9.63; Mn, 7.46%. FT-IR (KBr, cm^{-1}): 1592.79 (ν C=N); 1244.41 (ν C-O); 1013.39 (ν C-N-C). ^1H NMR (400 MHz, $CDCl_3$), δ (ppm): 16.465 (s, Ar-OH); 8.638-6.836 (m, Ar-H); 3.927 (t, N-CH_2); 3.264 (t, -CH_2-Ar); 2.311 (s, -CH_3). UV-Vis λ_{max} (nm) (CH_3OH): 214; 235; 277; 322; 372; 436; 490.

RESULT AND DISCUSSION

The Schiff base ligand was created via condensation of HAN and 4-chlorophenyl ethylamine. Schiff base ligand binds to transition metal ions Au (III), Pd (II), Cu (II), Fe (II), and Mn (II) to produce stable-coloured complexes. These compounds were soluble in typical polar solvents, including CHCl3, CH2Cl2, DMSO, DMF, and acetone. Analytical results validated the structure of the generated compounds. The compounds were tested for antibacterial activity against E. coli, P. aeruginosa, and S. aureus microorganisms, as well as antifungal activity against C. albicans and A. niger, and antioxidant activity was measured using the DPPH (2,2-Diphenyl-1-Picryl Hydrazyl) radical scavenging assay.

Spectroscopic studies

UV-Vis. spectra

Electronic absorption spectra of ligands and metal complexes are shown in Fig. 1, 2. Au (III), Pd (II), Cu (II), Fe (II) and Mn (II) metals are show coordination between ligand HL and metals to form complexes (Table 1). The UV-Vis spectra of the ligand's two aromatic rings revealed strong bands at 225, 272, and 287 nm, corresponding to the π→π* transition. At n → π* nonbonding aromatic -OH and imine -C=N- lone pair electrons produced strong bands at 322 nm and 409 nm respectively [40]. Metal complexes exhibit a shift in the electronic absorption band towards lower energy, i.e., higher wavelength 322 nm, 328 nm, 339 nm, 372 nm which is attributed to the ligands' phenolic -OH and imine -C=N- groups. Bands at higher wavelengths 433 nm, 462 nm, 484 nm, 541 nm, 573 nm indicate d → d transitions in complexes.

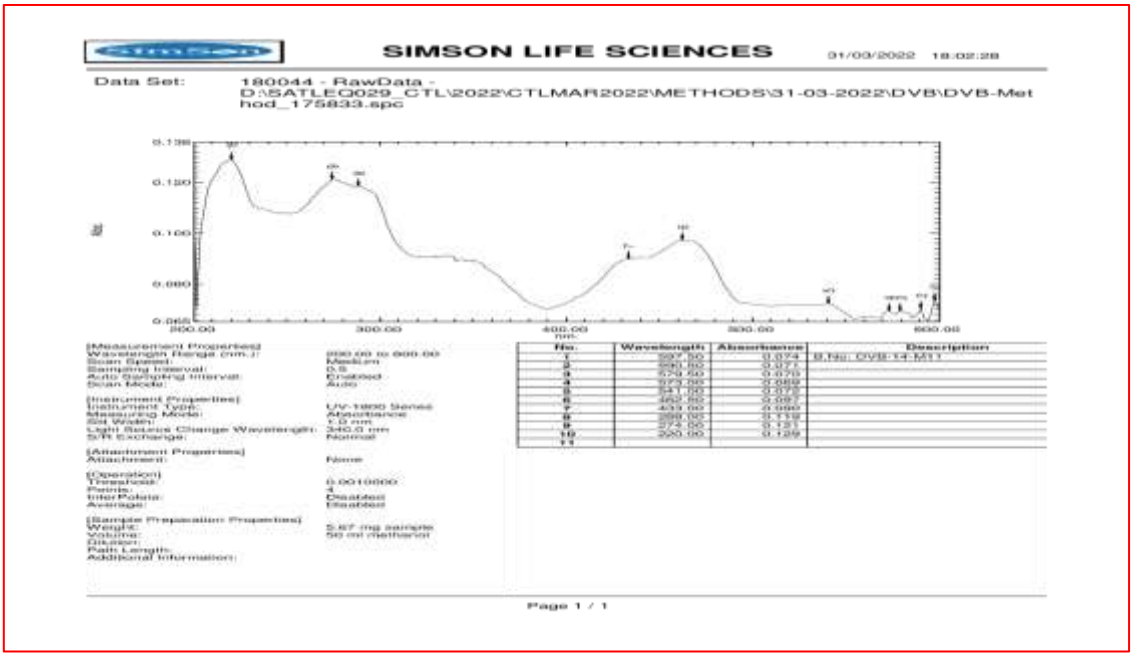

Figure 1: UV-Vis Spectra of Au (III) metal complex

ISSN: 0975-8585

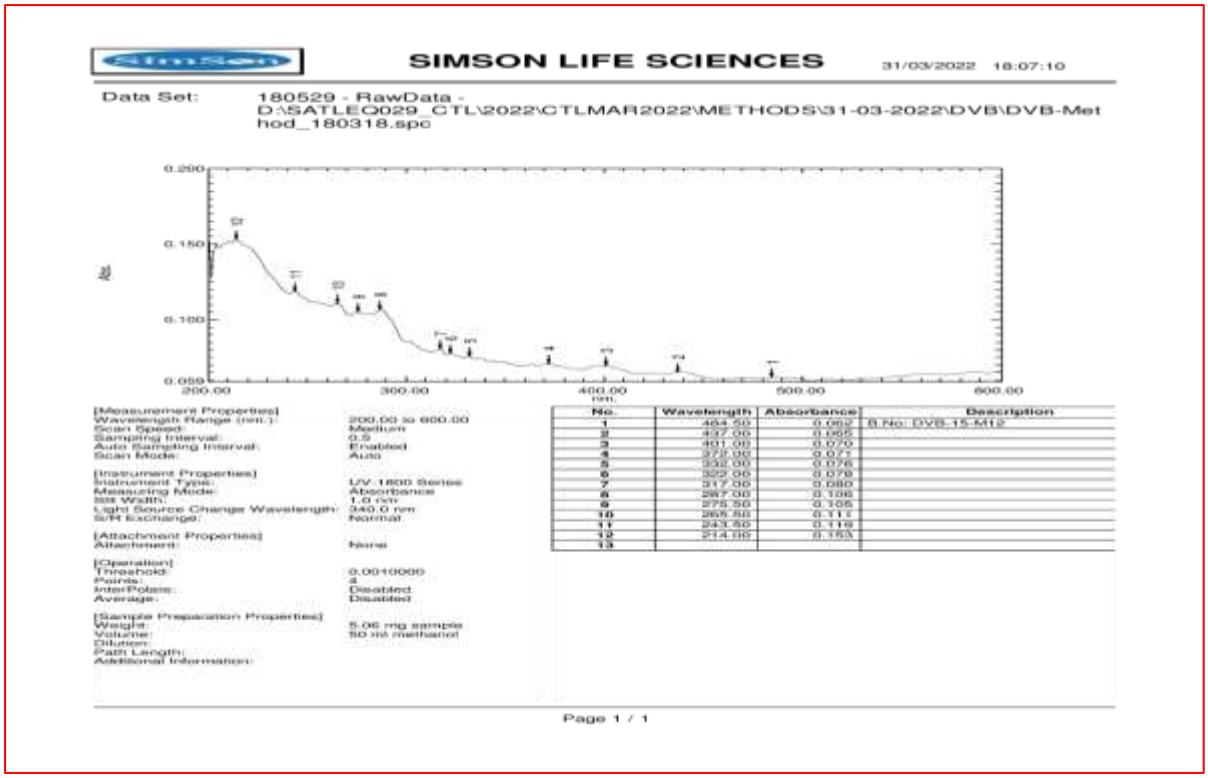

Figure 2: UV-Vis Spectra of Pd(II) metal complex

Table 1 - Electronic spectral assignments (λ) of Schiff base HL ligand and their complexes

Compounds	Electronic absorption bands and their assignments **(nm)**		
	π → π*	n → π*	Metal Ligand Charge Transfer transition (MLCT), d-d transition
HL	222 271.50 287.50	322.50 409.50s	--
$Au(L)_2$	220, 274	339	433, 462, 541, 573
$Pd(L)_2$	214, 243, 287	322, 372	437, 484
$Cu(L)_2$	221, 271, 286	328	407, 436
$Fe(L)_2(H_2O)_2$	220, 272, 288	322	409, 439
$Mn(L)_2(H_2O)_2$	223, 278, 292	322	412, 434

Magnetic susceptibility and molar conductance

Magnetic susceptibility measurements are widely used in studying transition metal complexes. The magnetic susceptibility and conductivity measurements of complexes Au(III), Pd(II), Cu(II), Fe(II) and Mn(II) are given in Table 2. The magnetic properties are there due to the presence of unpaired electrons in the partially filled d-orbital in the outer shell of these elements. These magnetic measurements give an outline about the electronic state of the metal ion in the complexes. The magnetic moment value of complex $Au(L)_2$ was approximately 0.21 B.M. and denoted as diamagnetic for low spin d^8 complexes and the geometry of Au(III) metal centre was square planar [41]. Conductivity measurements show Au(III) complex value is 10. The electrolytic nature of Au(III) complex suggests that non-ionic. This was supported by the 10 $\Omega^{-1}cm^2mol^{-1}$ conductance of Au(III) complex. The magnetic moment for $Pd(L)_2$ metal complex is 0.18 B.M. which showed that the Pd(II)complex to be with low spin d^8, diamagnetic and square planar. Conductivity measurements showed complex was non-ionic. The magnetic moment of $Cu(L)_2$ complex was found around 1.77 B.M., which is very consistent with indicative of one unpaired electron of Cu (II) ion in d^9 system and show distorted square planar geometry. The magnetic susceptibility measurement showed that the prepared $Fe(L)_2(H_2O)_2$ complex have paramagnetic character and having

high spin value 5.05 B.M. which indicates Fe(II) metal complex was exhibited low t_2g and eg in d^6 slitting of octahedral structure. The magnetic moment of $Mn(L)_2(H_2O)_2$ complex was found around 5.82 B.M., so Mn(II) complex was indicating d^5, it was high spin type paramagnetic and it lies in the octahedral structure. The molar conductance values of all these metal complexes were in the range 10 to 20 $\Omega^{-1}cm^2mol^{-1}$. These values were too low to account for any dissociation of the complexes in DMF. Hence, Au(III), Pd(II), Cu(II), Fe(II) and Mn(II) complexes can be regarded as non-electrolytes [42].

Table 2 - Magnetic moment and molar conductance data of metal complexes in DMF

Compounds	Magnetic moment μ_{eff} (B.M.)		Molar Conductance $\Lambda_m\Omega^{-1}cm^2mol^{-1}$	Proposed structure
$Au(L)_2$	0.21	Diamagnetic	10	Square planar
$Pd(L)_2$	0.18	Diamagnetic	12	Square planar
$Cu(L)_2$	1.77	Paramagnetic	20	Distorted square planar
$Fe(L)_2(H_2O)_2$	5.05	Paramagnetic	18	Octahedral
$Mn(L)_2(H_2O)_2$	5.82	Paramagnetic	15	Octahedral

FT-IR spectra

Important FT-IR vibrational bands of ligand and metal Au(III), Pd(II), Cu(II), Fe(II) and Mn(II) complexes demonstrate ligand coordination in Fig. 3, 4 (Table 3). In the IR spectra of HL ligand, a peak at 3424.77 cm^{-1} stretching was assigned to an intramolecular phenolic (ν OH) in the Naphthene ring of the Schiff base ligand [43]. Another weak band at 3045.8914 -2866.84 cm^{-1} is caused by the aromatic ring and aliphatic -C=C-H, -C-H stretching. The key vibrational band of imine -C=N- is detected at 1701.15 cm^{-1} and the shifting of higher wave number of imine group in Schiff base was observed as a result of intramolecular hydrogen bonding which effects electron density of imine groups. Other bands of ligand show at 1591.42- 1455.73 cm^{-1}, 1271.88 cm^{-1}, 1016.67 cm^{-1} are assignable to an aromatic ring (ν Ar C=C), phenolic (ν C-O) and ethyl chain imine (ν C-N-C) respectively.

In the FT-IR spectra of metal complexes, broad medium intensity peak 3424.77 cm^{-1} disappears, indicating that the phenolic (ν OH) group deprotonates in metal chelates and coordinates with metal ions. Peak at 3441.03- 3417.64 cm^{-1} is assigned of metal coordinated water (ν H_2O) in metal complexes. Imine peak of ligand is shifted to a lower wavenumber for Au(III) metal 1592.27 cm^{-1}, Pd(II) metal 1618.05, Cu(II) metal 1618.18 cm^{-1} and for Fe(II) metal broad peak 1588.36 cm^{-1}, Mn(II) metal broad peak 1592.79 cm^{-1} these broad peaks are observed it contains imine group peak which unite in that specific broad peak, this designates nitrogen of imine group coordinated in chelate formation. The IR peak of ligand 1271.88 cm^{-1} (ν C-O) was displaced 30 - 70 cm^{-1} upward in metal chelates due to oxygen electron delocalization toward metal atoms. According to the FT-IR data, the ligand's phenolic -OH acts as a bidentate and coordination takes place *via* imine nitrogen and the phenolic oxygen of the naphthalene ring in metal complexes.

ISSN: 0975-8585

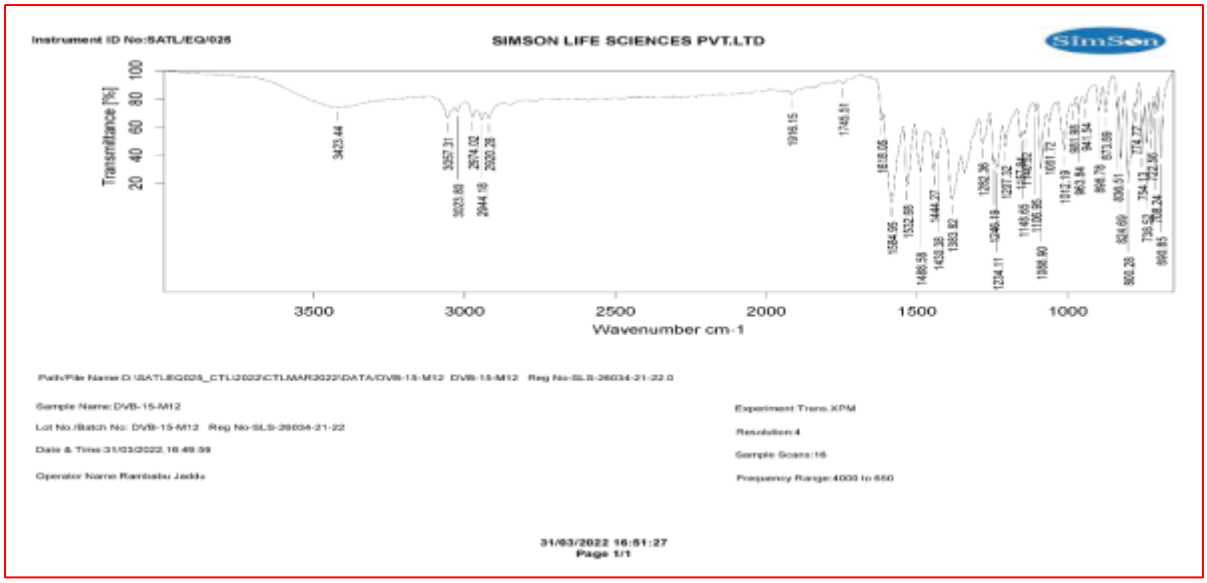

Figure 3: IR Spectra of Pd(II) metal complex

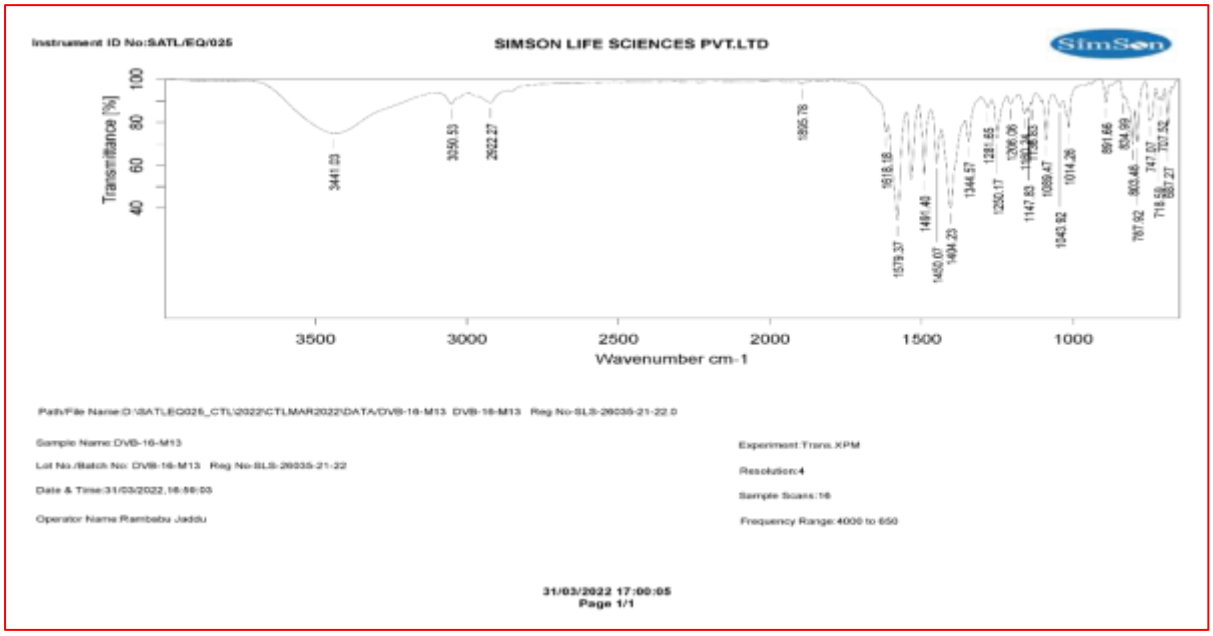

Figure 4: IR Spectra of Cu(II) metal complex

Table 3 - FT-IR spectral frequencies (4000 - 650 cm^{-1}) of Schiff base HL and their complexes

Compound	ν(-OH)	ν(H_2O)	ν(C=C–H)	ν(C=N–)	ν(C–O)	ν(C-N-C)
HL	3424.77	-	3045.8914	1701.15	1271.88	1016.67
$Au(L)_2$	-	3427.48	2923.75	1592.27	1246.55	1020.52
$Pd(L)_2$	-	3423.44	3057.31	1618.05	1246.19	1012.19
$Cu(L)_2$	-	3441.03	3050.53	1618.18	1250.17	1014.26
$Fe(L)_2(H_2O)_2$	-	3417.64	2929.57	1588.36	1271.69	1014.88
$Mn(L)_2(H_2O)_2$	-	3418.27	3056.35	1592.79	1244.41	1013.39

^{1}H NMR spectra

The ^{1}H NMR spectra of the free Schiff base ligand and its metal complexes were recorded in $CDCl_3$ solvent, as shown in supplementary material Fig. 5, 6 (Table 4). The structure of the Schiff base ligand

ISSN: 0975-8585

was in good accord with the various chemical shifts of the NMR spectrum. Deshielded tiny singlet peak was seen at 16.465 ppm due to phenolic -OH, which contains intramolecular hydrogen bonding and a more acidic proton [44]. Aromatic ring protons Ar-H confirm findings in the predicted range of 6.789-8.524 ppm. Another triplet peaks at 3.786 and 3.068 are assigned to -N=CH_2- CH_2-Ar respectively. Singlet peak at 2.268 is assigned to N=C-CH_3. The absence of the phenolic -OH band in the ^{1}H NMR spectra of transition metal complexes confirms that the -OH group deprotonated and coordinated with the metal to create the complexes. Chemical shift causes ppm values of other proton peaks that influence bonding in metal chelates to shift towards the downfield side.

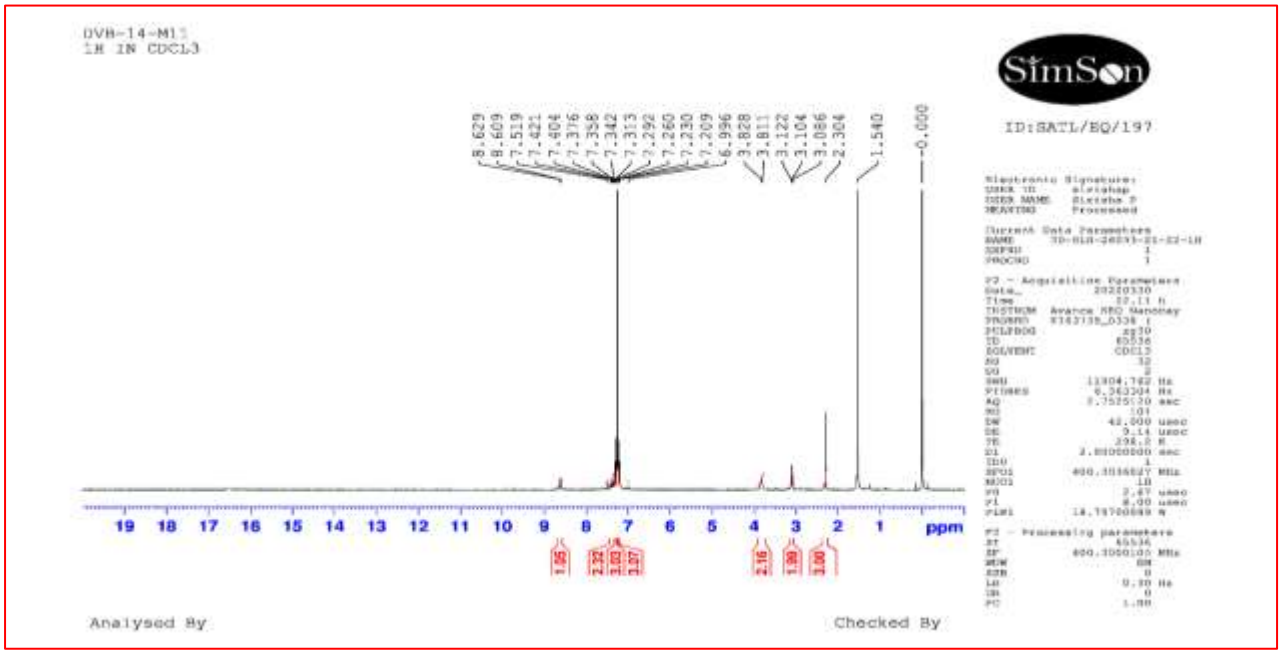

Figure 5: ^{1}H-NMR Spectra of Au(III) metal complex

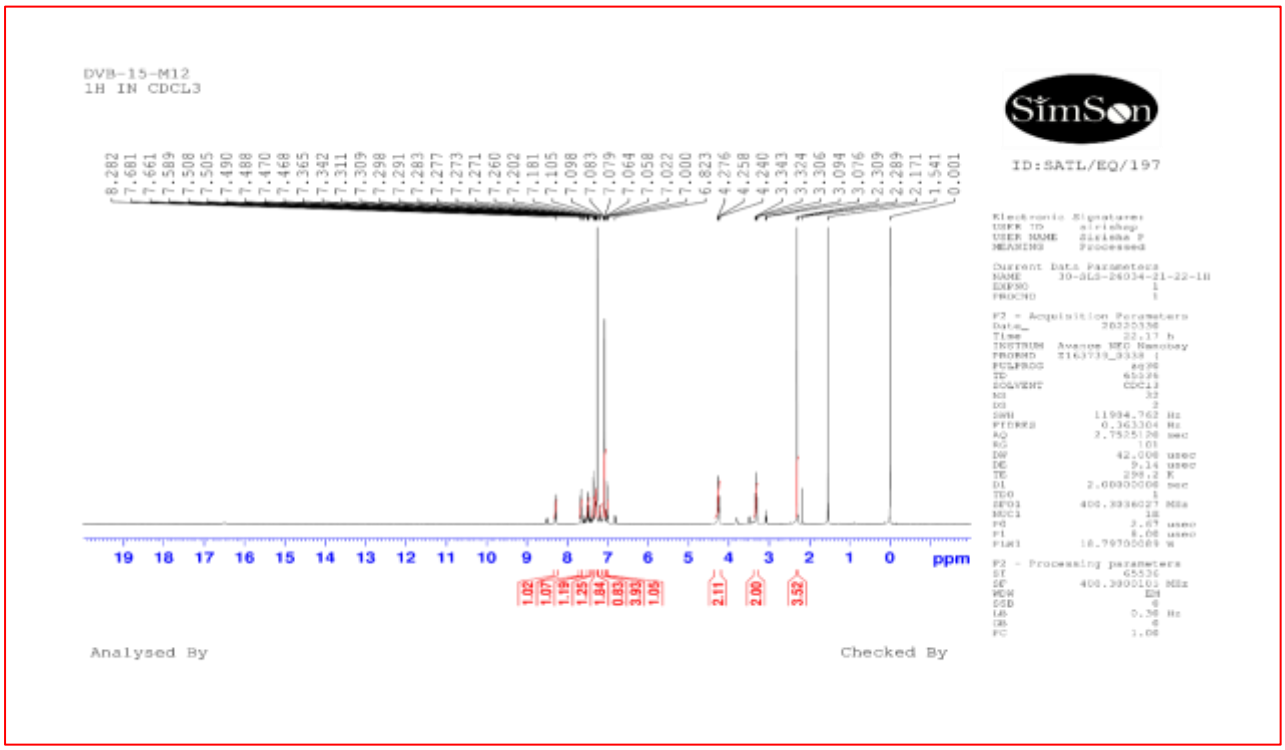

Figure 6: ^{1}H-NMR Spectra of Pd(II) metal complex

ISSN: 0975-8585

Table 4 - Spectroscopic data (^{1}H NMR) (δ) of the given Schiff base and its metal complexes

Compound	Ar-O<u>H</u>(s)	Ar-<u>H</u>(m)	-N-C<u>H</u>$_2$(t)	-C<u>H</u>$_2$-Ar(t)	-N=C-C<u>H</u>$_3$(s)
HL	16.465	6.789- 8.524	3.786	3.068	2.268
Au(L)$_2$	-	6.996- 8.629	3.828	3.122	2.304
Pd(L)$_2$	-	6.823- 8.282	4.276	3.343	2.309
Cu(L)$_2$	-	6.511- 8.953	3.818	3.097	2.314
Fe(L)$_2$(H$_2$O)$_2$	-	6.799- 8.523	3.832	3.094	2.307
Mn(L)$_2$(H$_2$O)$_2$	-	6.836- 8.638	3.927	3.264	2.311

LCMS

Mass spectral figure is shown in Fig. 7. FIA-Mass spectrometry was successfully employed to identify the molecular ion peak for a new Schiff base ligand ($C_{20}H_{18}ClNO$) at *m/z* 324.1. In the mass spectra of Schiff base HL recorded 324.1[M^+ + 1], 326.1[M^+ + 2] two isotopic peaks with the ratio of 1:3 intensity it is confirmed Chlorine atom in molecules. The peak was found in good agreement with the anticipated structure of the Schiff base ligand. Furthermore, metal complexes showed their expected molecular ion peaks, which included a Schiff base ligand peak; when mass spectra were collected, one of the ligand moieties is fractured from the complex.

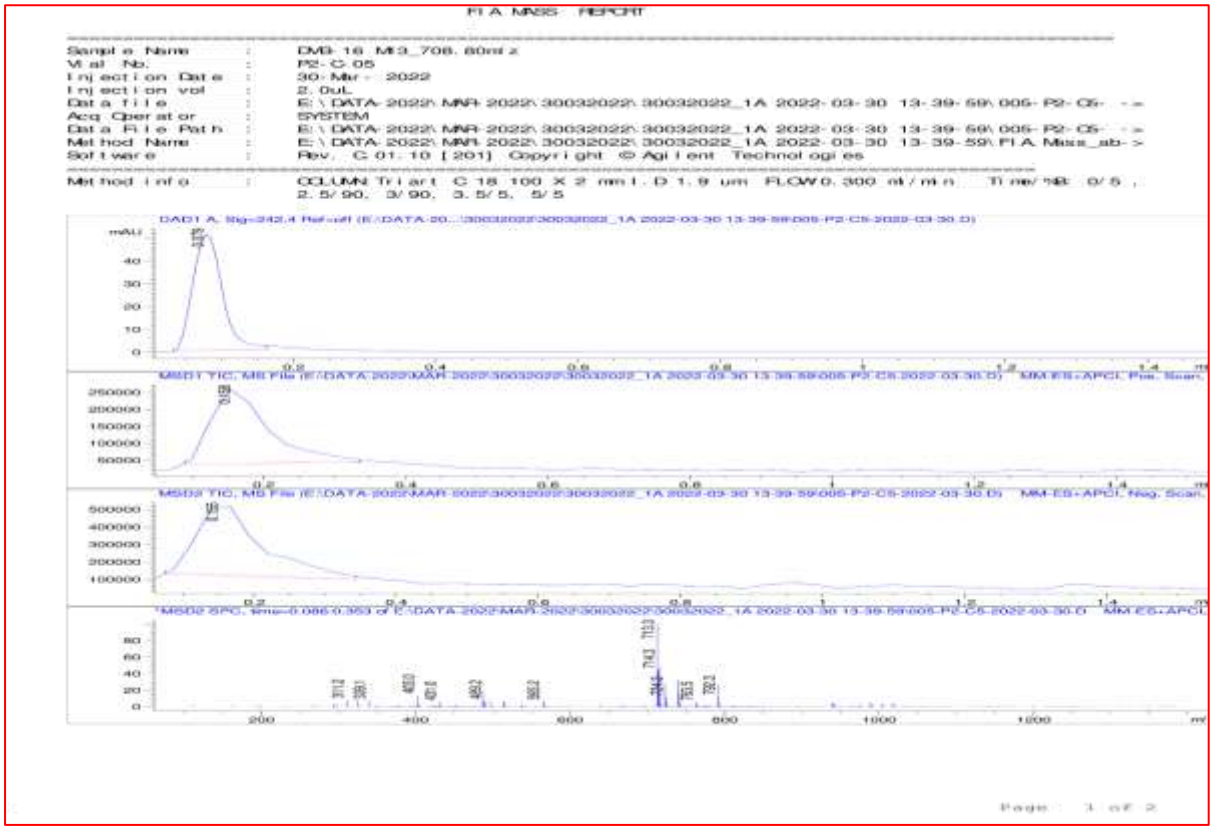

Figure 7: LCMS Spectra of Cu(II) metal complex

XRD

X-ray powder diffraction study was performed using an X-ray powder diffractometer with the following parameters: scanning mode- 2θ/θ, scanning type- continuous with a scan speed of 5.000 degrees/min, X-ray- Cu/ 30 kV / 15 mA, fixed monochromator with a 2θ range of 10 to 80 degrees and a sample width of 0.020 degrees. The synthesized ligand and its complex were assigned precise X-ray peaks, which aided in the comparison of reported spectra using the peak matching technique. Some of the new peak sites occur at higher intensities across all complexes, indicating that the metal ions were coordinated with the ligand. The peaks intensities of Schiff base at 13.909, 18.146, 19.728, 21.418, 23.980,

ISSN: 0975-8585

25.205, 27.709, 29.801, 33.944 region are abridged in all chelates which suggest the above practicality. Furthermore, larger peaks in all complexes demonstrate Schiff base coordination in complexes caused by the binding of donor oxygen and nitrogen atoms to metal ions. The ligand and complexes, as well as their crystal system, space group and unit cell volume parameters are produced by the calculation and are displayed in Table 5. Schiff base ligand and complexes X- ray graphs are shown in Fig. 8, 9.

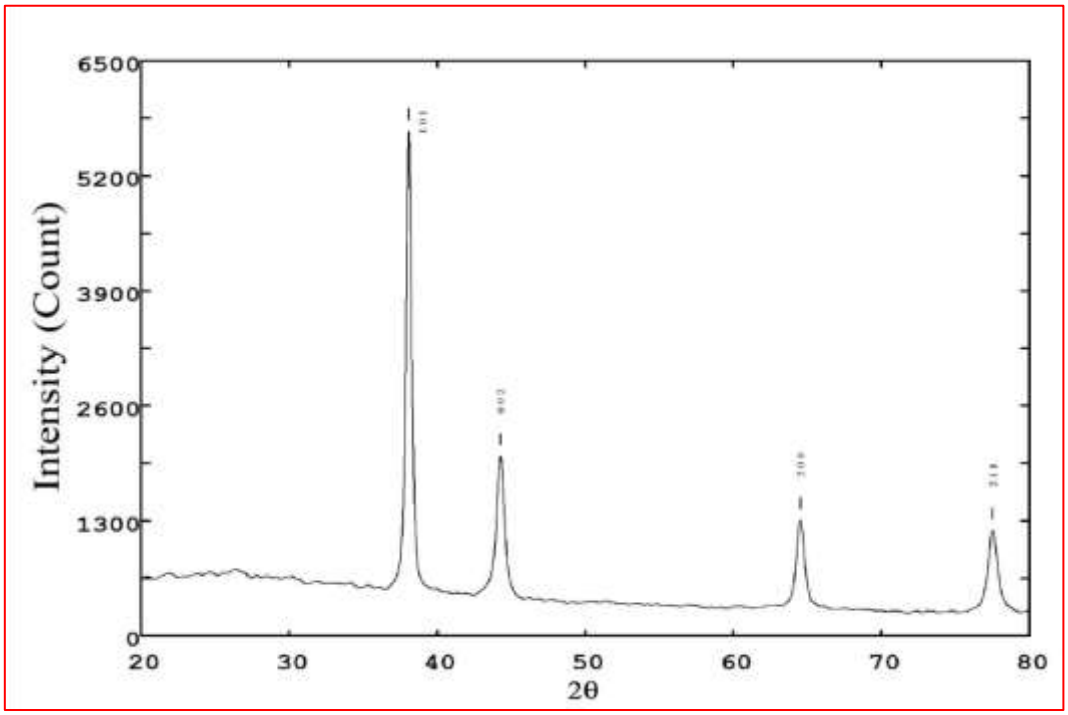

Figure 8: XRD Spectra of Au(III) metal complex

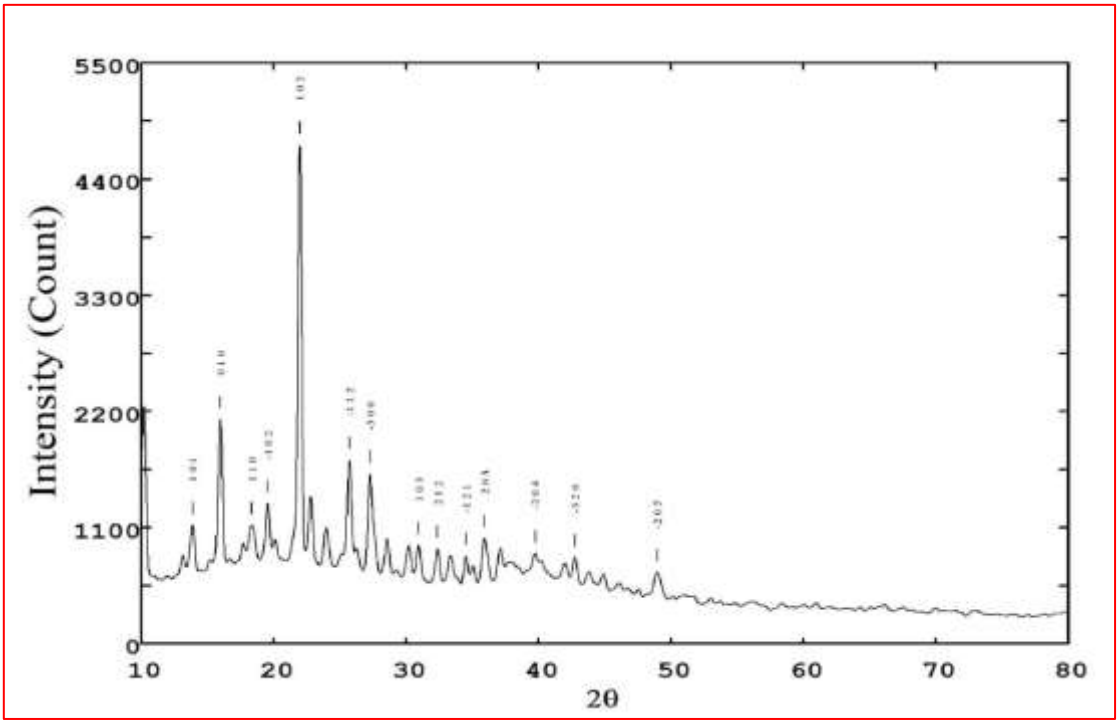

Figure 9: XRD Spectra of Pd(II) metal complex

Table 5 - X-ray powder diffraction data of the given Schiff base and its metal complexes

Compound	HL	$Au(L)_2$	$Pd(L)_2$	$Cu(L)_2$	$Fe(L)_2(H_2O)_2$	$Mn(L)_2(H_2O)_2$
Empirical formula	$C_{20}H_{18}ClNO$	$C_{40}H_{34}AuCl_2N_2O_2$	$C_{40}H_{34}Cl_2N_2O_2Pd$	$C_{40}H_{34}Cl_2CuN_2O_2$	$C_{40}H_{38}Cl_2FeN_2O_4$	$C_{40}H_{38}Cl_2MnN_2O_4$
Formula weight	323.824	842.59	752.04	709.17	737.50	736.59
Temperature, K	298	298	298	298	298	298
Crystal system	Triclinic	Tetragonal	Monoclinic	Monoclinic	Orthorhombic	Orthorombic
Lattice type	*P1*	*P 2/m*	*P 2₁/c*	*P 2/m*	*P mmm*	*P mmm*
a/A°	6.6059(7)	2.885526	9.906397	12.81334	17.383476	12.80153
b/A°	7.6344	2.885526	5.547025	8.575715	16.770363	8.951424
c/A°	9.7623	4.088921	9.578026	8.730887	3.338842	5.277690
α/°	67.457	90.00000	90.000000	90.000000	90.000000	90.000000
β/°	82.004	90.00000	98.24286	127.3318	90.000000	90.000000
γ/°	64.855	90.00000	90.000000	90.000000	90.000000	90.000000
Unit cell volume, $A^{\circ 3}$	411.46	834.04542	820.88512	762.83929	973.36	604.78061

Biological activity of Schiff base HL and their metal complexes

Antimicrobial activity (antibacterial, antifungal)

The antibacterial activity was assessed *in vitro* using the Zone Inhibition Method. The Mueller Hinton Agar (MHA) plates were spread and inoculated with 100 µL of log cultures of all microorganisms (adjusted to 0.5 McFarland Unit). Compound concentrations of 10 µg/disc were loaded onto 5 mm sterile individual discs. One disk in each plate was filled with solvent alone, which served as a vehicle control DMSO and *Ciprofloxacin* (2 mg/mL, 20 µg) was used as a positive control. Plates of test organisms were cultured at 37°C for 24 h and clear zones formed around the disc were measured and recorded in millimetres. Schiff bases and complexes were tested for antibacterial activity against pathogenic gram-negative bacteria *Escherichia coli*, *Pseudomonas aeruginosa* and gram-positive *Staphylococcus aureus*, *Bacillus subtilis*, using *Ciprofloxacin* as a positive control and the solvent DMSO as a negative control, with the results shown in Table 6 and graphical representation is shown in Figure 10. However, all of the chemicals studied have more bacterial activity against gram-positive than gram-negative infections. Gram-positive bacteria can easily absorb antibiotics and cleaning chemicals because of their thicker peptidoglycan coating. However, because of their thin peptidoglycan covering, gram-negative bacteria are immune to certain physical attacks since they do not absorb foreign substances that surround them. The chlorophenyl group, an electron acceptor group with a lowest spatial barrier was discovered to have antibacterial action in HL. Stronger electron acceptors demonstrate better antibacterial activity [45, 46]. Complexes may perform better than free Schiff bases because their reduced polarity makes it easier for them to cross cell membranes. Based on the Overtone concept [47] and Tweedy's chelation theory [48], this behaviour can be explained by the formation of coordinate covalent bonds. This activity is linked to the formation of coordinating covalent bonds. We found that when Schiff base ligands are coupled in chelate form with metals, their antibacterial activity rises. Among these, Au(III) and Pd(II) metal complexes have moderate antibacterial activity compared to other metals.

In vitro, the antifungal activity of Schiff base ligands and complexes was investigated against the fungal species *Candida albicans* and *Aspergillus niger* which were cultivated on potato dextrose agar. This antifungal activity was determined using the disc diffusion method and the findings are shown in Table 6 and graphical representation is shown in Fig. 10. The chemical solutions were produced in DMSO and soaked on a filter paper disk measuring 5 mm in diameter and 1 mm thick. The plates of test fungus were cultured at 37°C for 72 h and the vivid zones formed around the disc were measured and recorded in millimetres. Furthermore, during coordination, π-electrons delocalize over the chelate ring system created by the donor groups, increasing the lipophilicity of the complexes. Leading to the ability to penetrate the microorganism's lipid is coating, resulting in more efficient death [49]. Schiff base ligands and metal complexes outperform *ciprofloxacin* as a reference medication in antifungal studies.

ISSN: 0975-8585

Furthermore, when HL ligands are chelated with metals, their antifungal bioactivity rises. In between these metal complexes, Au(III) and Pd(II) showed significant antifungal activity.

Table 6 - Antibacterial and Antifungal activity data of Schiff base and its metal complexes (in mm)

Compound	Concentration µg/mL	Antibacterial activity				Antifungal activity	
		E. coli	*P. aeruginosa*	*S. aureus*	*B. subtilis*	*C. albicans*	*A. niger*
HL	1000	12	10	14	11	8	9
	500	10	11	12	10	6	8
	250	9	8	9	9	5	7
	125	8	6	8	7	-	5
	50	6	6	5	5	-	-
$Au(L)_2$	1000	18	20	19	17	13	11
	500	15	16	14	15	9	10
	250	13	12	10	12	6	8
	125	9	10	7	10	6	7
	50	7	6	5	6	5	6
$Pd(L)_2$	1000	19	21	20	19	13	11
	500	14	14	14	15	11	10
	250	9	11	10	10	7	7
	125	9	9	7	8	6	5
	50	6	5	7	5	5	5
$Cu(L)_2$	1000	14	12	15	14	10	11
	500	11	10	11	12	9	9
	250	10	9	8	10	7	7
	125	7	8	6	8	6	7
	50	-	7	-	5	-	-
$Fe(L)_2(H_2O)_2$	1000	13	14	14	11	11	10
	500	10	10	9	10	9	8
	250	7	8	6	8	6	6
	125	6	7	6	5	6	5
	50	-	-	-	-	-	-
$Mn(L)_2(H_2O)_2$	1000	15	13	16	14	10	11
	500	12	10	10	11	9	10
	250	7	8	9	10	7	7
	125	6	7	6	8	6	6
	50	5	5	6	6	5	5
*Ciprofloxacin**	20	39	31	33	28	5	5

* Standard reference drug

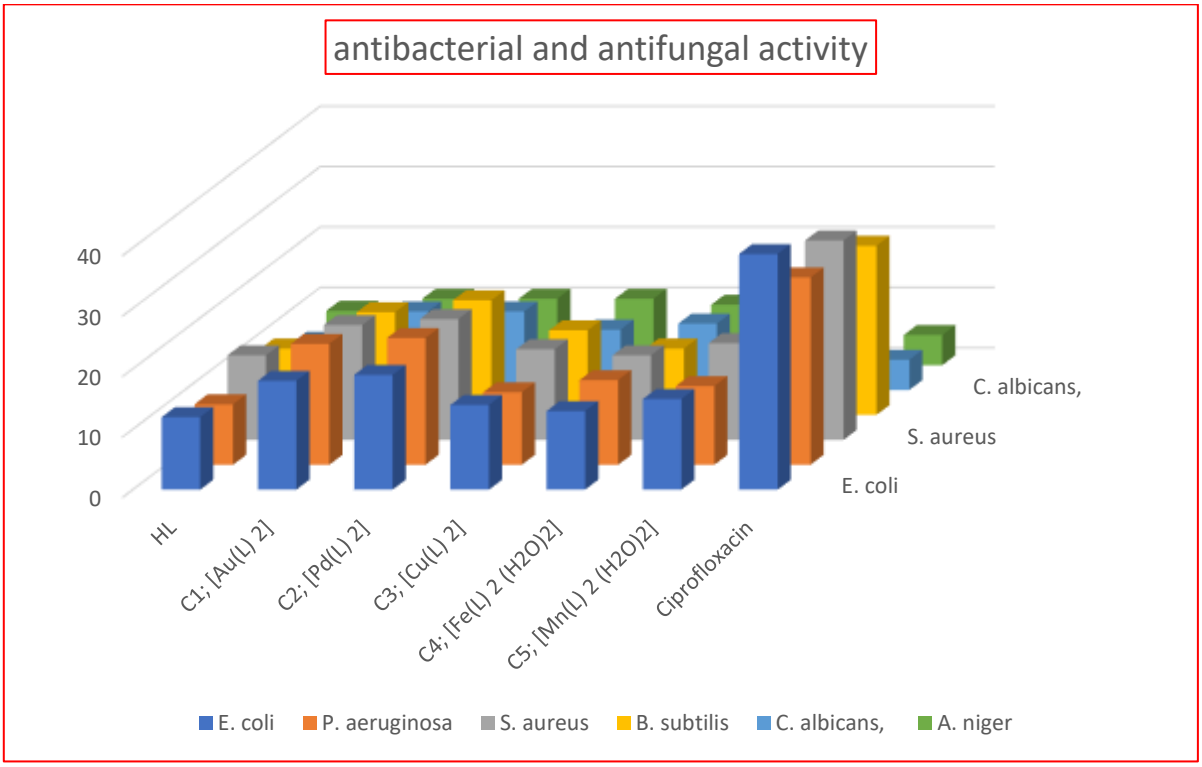

Figure 10: - Graphical representation of antibacterial and antifungal activity data of Schiff base HL and its metal complexes for 1000 µg/mL (in mm)

Antioxidant activity

According to the reputable method 2,2-diphenyl-1-picrylhydrazyl radical scavenging assay was used to estimate the antioxidant activities of the synthesized compounds. The test solution containing a mixture 5µl of different stock of the test compound (10µg/ml-2500 µg/ml) was added to 0.1 ml of 0.1mM DPPH solution in a 96 well plate. The reaction was set in triplicate form and duplicates of blank was prepared containing 0.2 ml DMSO/Methanol and 5µl compound of different concentrations (10µg/ml-2500 µg/ml). The plate was incubated for 30 min in dark. At the end of the incubation, the decolorization was read 495 nm using a micro plate reader (iMark, BioRad). Reaction mixture containing 20 µl of deionized water was served as Control. The scavenging activity was presented as '% inhibition' with respect to control.

$$\text{DPPH Scavenging activity} = ((\text{Abs}_{\text{Control}} - \text{Abs}_{\text{Sample}})/\text{Abs}_{\text{Control}}) \times 100$$

The antioxidant activity of the Schiff base ligand and metal complexes was measured using the DPPH technique and compared to that of standard *Ascorbic Acid*. The results of the free radical scavenging activity of synthesized compounds at various concentrations are reported in Table 7 and a graphical depiction is shown in Figure 11. Metal complexes demonstrated more activity than the free Schiff base. Metal ions' capacity to remove electrons promotes the release of hydrogen and reduces DPPH radicals, resulting in increased antioxidant activity [50]. Pd(II) complexes have demonstrated more scavenging activity than Au(III) and Cu(II) complexes.

ISSN: 0975-8585

Table 7 - Antioxidant activity of synthesized Schiff base HL and its complexes

Conc. [µg/mL]	*Ascorbic acid**	HL	$Au(L)_2$	$Pd(L)_2$	$Cu(L)_2$	$Fe(L)_2(H_2O)_2$	$Mn(L)_2(H_2O)_2$
% Inhibition							
10	16.9507	1.9528	2.8996	1.5528	0.8996	0.2447	1.6973
50	16.4126	4.6113	3.2965	2.3519	1.1537	0.2966	3.4421
100	32.6457	7.6439	8.3294	8.4613	1.1995	1.9572	7.5538
250	61.1659	9.2218	12.5527	19.2311	2.7231	2.7613	10.8911
500	75.6951	11.3624	17.6914	25.8429	5.8724	3.5184	26.1284
1000	88.1614	14.8457	23.6118	57.6772	7.7981	3.8621	32.6921
2500	88.7892	15.9962	38.1258	96.6355	8.9377	4.6443	39.9627

* Standard reference drug

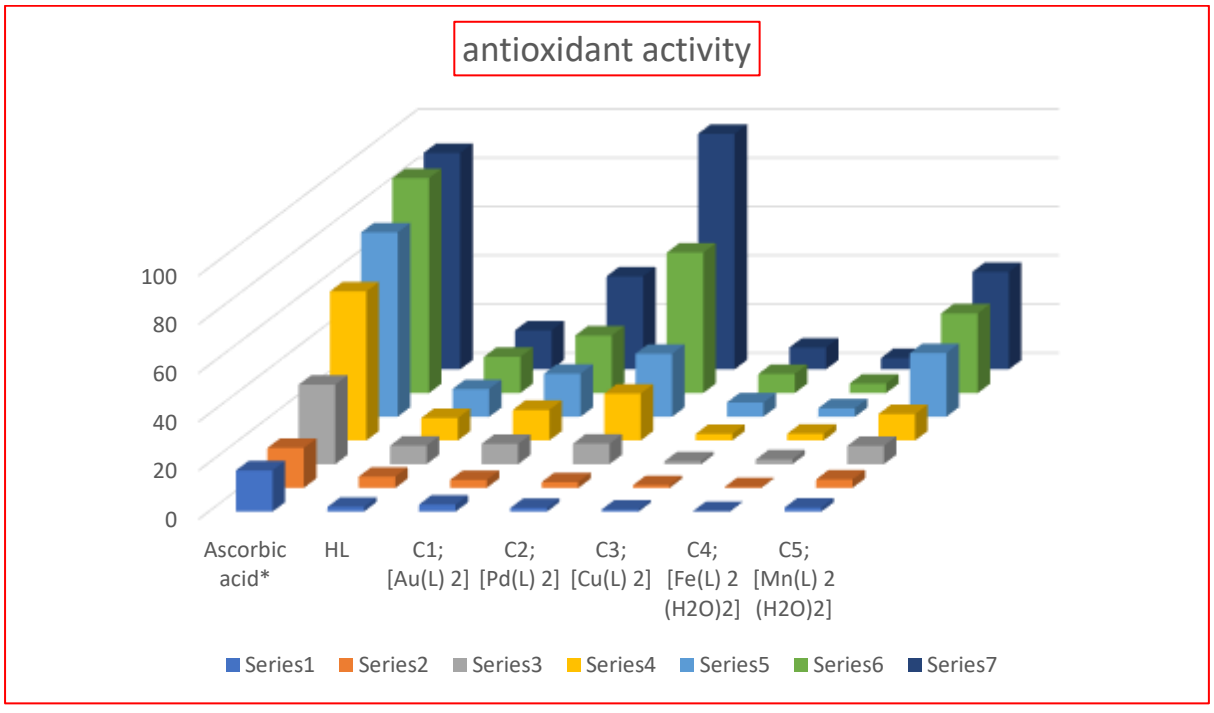

Figure 11: Graphical Representation of antioxidant activity data of Schiff base ligand and its metal complexes

CONCLUSION

In light of the aforementioned study, a number of Au(III), Pd(II), Cu(II), Fe(II), and Mn(II) complexes were synthesized using the unsymmetrical bidentate Schiff base ligand E-2-(1-((4-chlorophenethyl)imino)ethyl)naphthalen-1-ol. The presence of naphthol oxygen and azomethine nitrogen in the physicochemical data suggests that Au(III) and Pd(II) complexes have a square-planar geometry, Cu(II) complexes have a distorted square-planar geometry, and Fe(II) and Mn(II) complexes

have an octahedral geometry. All metal complexes exhibited stronger antibacterial and antifungal activities than their parent ligands. At a dosage of 2500 µg/mL, the Pd(II) metal complex outperforms the reference prescription Ascorbic acid for antioxidant activity. Based on all of these findings, it was determined that the bidentate N, O Schiff bases and their metal complexes provide significant and versatile information about coordination molecules, as well as the potential to be valuable biological agents.

ACKNOWLEDGMENTS

The authors would like to express their heartfelt gratitude to IIT Hyderabad for SC-XRD crystallographic analysis, LCMS spectral facility in University of Hyderabad and Simson Life Science, Hyderabad for ^{1}H NMR, ^{13}C NMR, FT-IR, and UV-Vis spectral facilities.

REFERENCES

[1] Uddin MN, Ahmed SS, Alam SMR. J Coord Chem 2020; 73: 3109-3149.
[2] Kargar H, Aghaei-Meybodi F, Elahifard MR, Tahir MN, Ashfaq M, Munawar KS. J Coord Chem 2021; 74: 1534-1549.
[3] Ortegón-Reyna D, Garcías-Morales C, Padilla-Martínez I, García-Báez E, Aríza-Castolo A, Peraza-Campos A, Martínez-Martínez F. Molecules 2014; 19: 459-481.
[4] Alamgholiloo H, Zhang S, Ahadi A, Rostamnia S, Banaei R, Li Z, Liu X. Shokouhimehr M. Mol Catal (2019); 467: 30-37.
[5] Kargar H, Torabi V, Akbari A, Behjatmanesh-Ardakani R, Sahraei A, Tahir M N. *J Mol Struct* 2020; 1205: 127642-127648.
[6] Vhanale BT, Shinde AT. J Iran Chem Soc 2022; 19: 2641-2653.
[7] Jana S, Bhaumik PK, Harms K. Chattopadhyay S. Polyhedron 2014; 78: 94-103.
[8] Lee JM, Shin SY, Yoon H, Lee MS, Lee YR, Koh D. Le YH. *J Korean Soc App. Biol Chem* 2013; 56: 343-347.
[9] Freitas VLS, da Silva MDMCR. Molecules 2020; 25: 3827-3841.
[10] Organero JA, Martin C, Cohen B, Douhal A. Langmuir 2008; 24: 10352-10357.
[11] Banik D, Kuchlyan J, Roy A, Kundu N, Sarkar N. J Phys Chem B 2015; 119: 2310-2323.
[12] Ardakani AA, Kargar H, Feizi N, Tahir M N. J Iran Chem Soc 2015; 15: 1495-1504.
[13] Pinna R, Jamme F, Rutten FJM, Smith EF, Willis MR, Briggs D, McCoustra MRS. Appl Surf Sci 2006; 252: 6672-6675.
[14] Shanty AA, Philip JE, Sneha EJ, Kurup MRP, Balachandran S, Mohanan PV. Bioorg Chem 2017; 70: 67-73.
[15] Sahraei A, Kargar H, Hakimi M, Tahir MN. Transit Met Chem, 2017; 42: 483-489.
[16] Rathelot P, Vanelle P, Gasquet M, Delmas F, Crozet M P, Timon-David P, Maldonado J. Eur J Med Chem 1995; 30:503-508.
[17] Sankar R, Sharmila TM. Results Chem 2023; 6: 101179.
[18] Ashok D, Padmavati K, Lakshmi BV, Sarasija M. Chem Heterocycl Compd 2016; 52: 15-20.
[19] da Silva CM, da Silva DL, Modolo LV, Alves RB, de Resende MA, Martins CVB, de Fa´tima A. J Adv Res 2011; 2: 1-8.
[20] Sriram D, Yogeeswari P, Myneedu NS, Saraswat V. Bioorg Med Chem Lett 2006; 16: 2127-2129.
[21] Soman SS, Soni JN, Patel TB. Med Chem Res 2014; 23: 3803-3809.
[22] Mir J M, Majid S A & Shalla A H, Rev Inorg Chem 2021; 41: 199-212.
[23] Ibrahim SRM, Mohamed GA. Phytochem Rev 2016; 15: 279-295.
[24] Jarrahpour A, Shirvani P, Sharghi H, Aberi M, Sinou V, Latour C, Brunel JM. Med Chem Res 2015; 24: 4105-4113.
[25] Sarasija M, Sudershan K, Ashok D, Shivaraj, Russ J Gen Chem 2014; 84: 1622-1628.
[26] Vhanale BT, Deshmukh NJ, Shinde AT. Heliyon 2019; 5: e02774-e02793.
[27] Singh JV, Mal G, Kaur G, Gupta MK, Singh A, Nepali K, Singh H, Sharma S, Bedi PMS. Med Chem Commun 2019; 10: 128-148.
[28] Ünlüer D, Ünver Y, Düğdü E, Alpaslan YB, Köysal Y, Soylu MS, Sancak K. Russ J Org Chem 2019; 55: 254-261.
[29] Song MK, Lee SJ, Kang YY, Lee Y, Mok H, Ahn JH. Appl Biol Chem 2017; 60: 597-602.
[30] Bougossa I, Aggoun D, Ourari A, Berenguer R, Bouacida S, Morallon E. Chem Pap 2020; 74: 3825-3837.

[31] Bergman J, Yasar S, Winger G. Psychopharmacology 2001; 159: 21-30.
[32] Özgeriş B. Monatsh Chem 2020; 151: 1851-1857.
[33] Simplício AL, Clancy JM, Gilmer JF. Molecules 2008; 13: 519-547.
[34] Raman N, Sobha S, Thamaraichelvan A, Spectrochim Acta A 2011: 78: 888-898.
[35] Ani FE, Ibeji CU, Obasi NL, Kelani MT, Ukogu K, Tolufashe GF, Ogundare SA, Oyeneyin OE, Maguire GEM, Kruger HG. Sci Rep 2021; 11: 8151-8162.
[36] Glennon RA. J Med Chem 2017; 60: 2605-2628.
[37] Alnoman MM, Parveen S, Alnoman RB, Khan A, Khaleil MM, Jaremko M, Younis IA, Emwas AH. J Mol Struct 2024; 1307: 138021-138030.
[38] Nguyen T, Gamage TF, Finlay DB, Deckar AM, Langston TL, Barrus D, Glass M, Li JX, Kenakin TP, Zhang Y. J Med Chem 2022; 65: 257-270.
[39] Rani P, Pal D, Hegde RR, Hashim SR. Biomed Res Int 2014; 2014: 1-9.
[40] Boghaei DM, Lashanizadegan M. Syn React Inorg Met Org Chem 2000; 30: 1393-1404.
[41] Prabhakara CT, Patil SA, Toragalmath SS, Kinnal SM, Badami PS. J Photochem Photobiol B 2016; 157: 1-37.
[42] Abou Melhaa KSA, Al-Hazmib GAA, Refat MS. Russ J Gen Chem 2017; 87: 3043-3051.
[43] Raman N, Thangraja C, Johsonraja S. Cent Euro J Chem 2005; 3: 537-547.
[44] Kumar A, Agarwal M, Singh AK. J Organomet Chem 2008; 693: 3533-3545.
[45] Lupas¸cu G, Pahonţu E, Shova S, Felicia Barbuceanu Ş, Badea M, Paraschivescu C, Neamţu J, Dinu M, Ancuceanu RV, Draganescu D, Dinu-Pîrvu CE. Appl Organomet Chem 2021; 35: 6149-6169.
[46] Kargar H, Ardakani AA, Tahir MN, Ashfaq M, Munawar KS. *J Mol* Struct 2021; 1233: 130112-130153.
[47] Anjaneyulu Y, Rao RP. Synth React Inorg Met-Org Chem 1986; 16: 257-265.
[48] Tweedy BG. Phytopathology 1964; 55: 910-914.
[49] Kargar H, Behjatmanesh-Ardakani R, Torabi V, Sarvian A, Kazemi Z, Chavoshpour-Natanzi Z, Mirkhani V, Sahraei A, Tahir MN, Ashfaq M. Inorg Chim Acta 2021; 514: 120004-1200045.
[50] Yadav M, Sharma S, Devi J. J Chem Sci 2021; 133: 21-43.